Figure legends

Figure 1. Construction of the *in vitro* dental cell co-culture systems.

Two dental cell lines were co-cultured in *in vitro* co-culture systems using a transparent collagen membrane. The two cell lines used were: a dental epithelial cell line (HAT-7) established from a cervical loop epithelium of a rat incisor, and a dental follicle cell line (BCPb8) established from the follicle tissue of a bovine incisor. The Sandwich co-culture (SW) method involved inoculation of HAT-7 cells into one side of a collagen film suspended in a culture dish, and inoculation of BCPb8 cells onto the opposite side of the same collagen film (B). The separate co-culture method (SC) involved seeding of BCPb8 cells onto a cell culture dish, followed by seeding of HAT-7 cells onto a collagen film in the same a dish, using the side of the film facing away from the BCPb8 cells (A)."

Figure 2. Sandwich co-culture of HAT-7 cells enhances Ameloblastin mRNA expression. The level of ameloblastin mRNA expression in HAT-7 cells grown in monolayer culture on a collagen membrane (white bars; ML), in the sandwich co-culture system (black bars; SW), or in the separate co-culture system (grey bars; SC) was analyzed. Total RNA was prepared from the cells at the indicated time points and was used for the synthesis of cDNA. The levels of ameloblastin mRNA expression were analyzed using real-time PCR and species-specific primers. Data were normalized to glyceraldehyde-3-phosphate dehydrogenase (GAPDH) mRNA expression levels in the same sample. Values are presented as means ± standard deviation (n=3). Error bars indicate the standard deviation of mean changes. Data were statistically analyzed using student t test. *$p<0.05$

Figure 3. Sandwich co-culture of HAT-7 cells enhances Amelogenin mRNA expression. The level of amelogenin mRNA expression in HAT-7 cells grown in monolayer culture on a transparent collagen membrane (white bars; ML), in the sandwich co-culture system (black bars; SW) or in the separate co-culture system (grey bars; SC) was analyzed. Total RNA was prepared from the cells at the indicated time points and was used for synthesis of cDNA. The levels of amelogenin mRNA expression were analyzed using real-time PCR and species-specific primers. Data were normalized to glyceraldehyde-3-phosphate.dehydrogenase (GAPDH) mRNA expression levels in the same sample. Values are presented as means ± standard deviation (n=3). Error bars indicate the standard deviation of mean changes. Data were statistically analyzed using student t test. *$p<0.05$

Figure 4. Sandwich co-culture of HAT-7 cells enhances Ameloblastin protein expression. Ameloblastin protein expression in sandwich co-cultured HAT-7 and BCPb8 cells was analyzed on days 1 (A), 3 (B), 7 (C) and 14 (D and E) of culture using immunofluorescence. On each day, HAT-7 cells were fixed and stained for ameloblastin (green) and nuclei were stained with Hoechst 33258 (blue). The cells were analyzed using a confocal laser scanning microscope. The image in E is a cross-sectional view of the 14 days sample. Ameloblastin protein expression was detected in HAT-7 cells (arrow in E) but not in BCPb8 cells (D). The expression of ameloblastin protein was detected in HAT-7 cells from day 3 of the sandwich co-culture with BCPb8 cells.

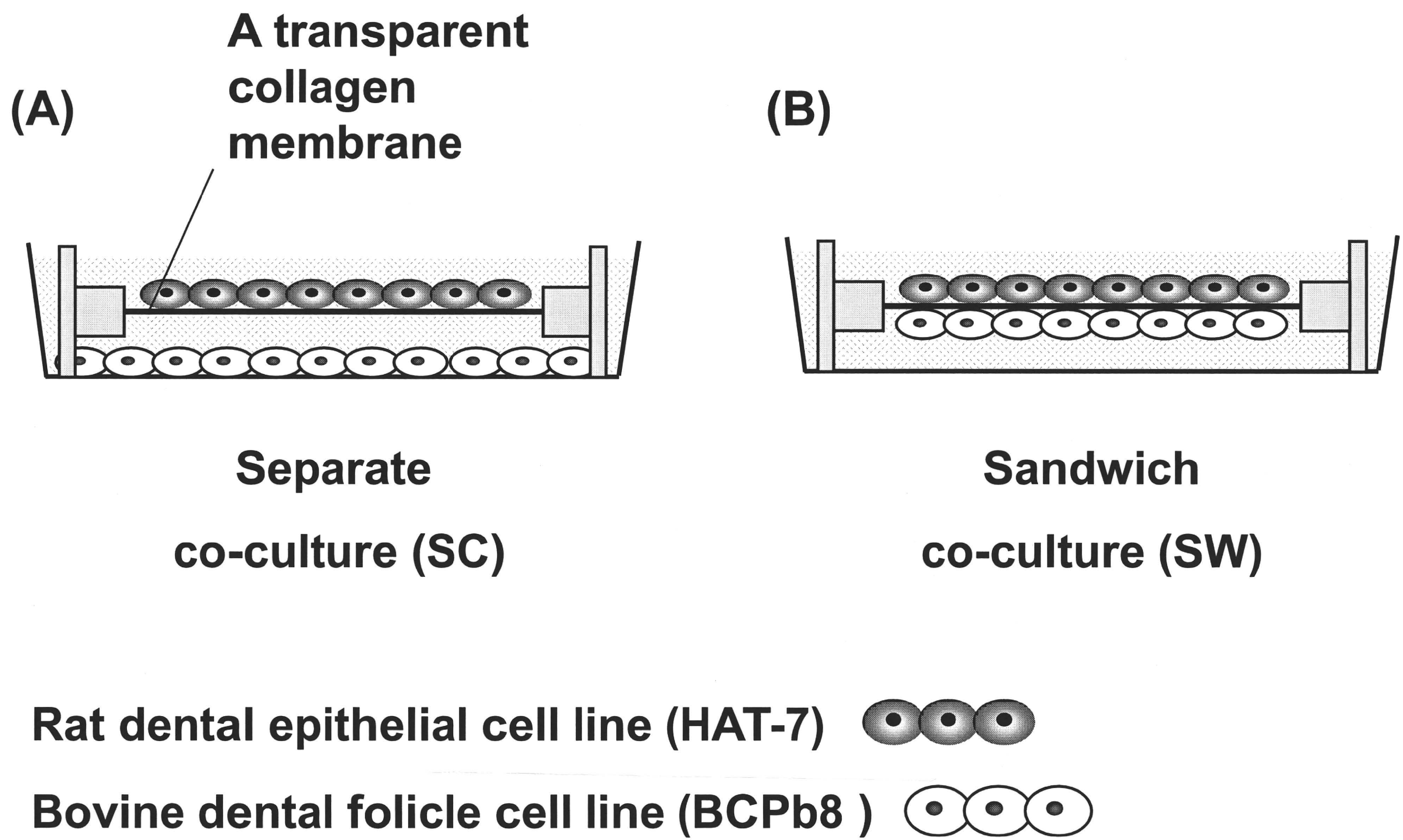
(A)
A transparent collagen membrane
Separate
co-culture (SC)
(B)
Sandwich
co-culture (SW)
Rat dental epithelial cell line (HAT-7)
Bovine dental folicle cell line (BCPb8)

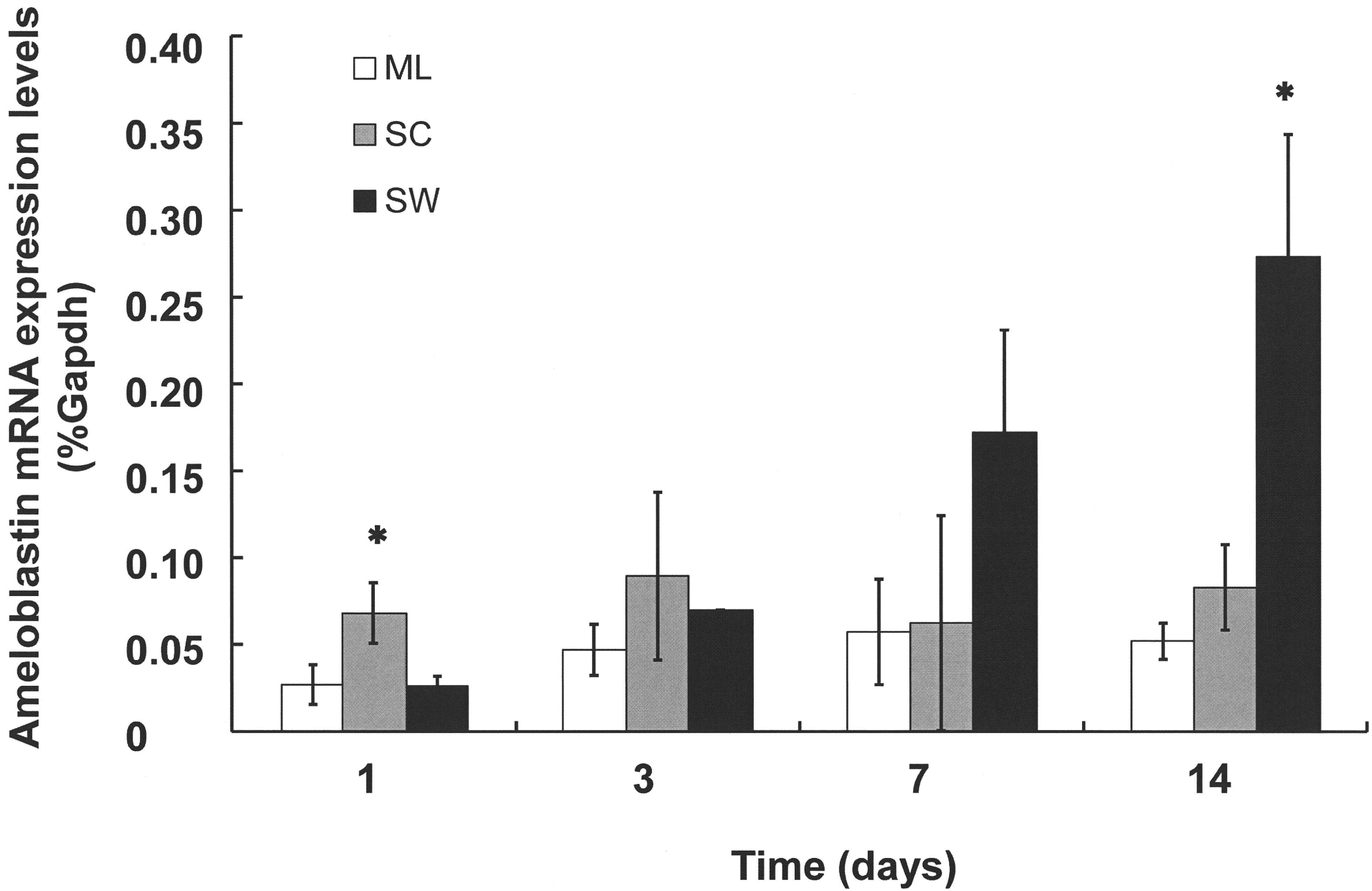
Ameloblastin mRNA expression levels (%Gapdh)
0.40
0.35
0.30
0.25
0.20
0.15
0.10
0.05
0
ML
SC
SW
*
*
1
3
7
14
Time (days)

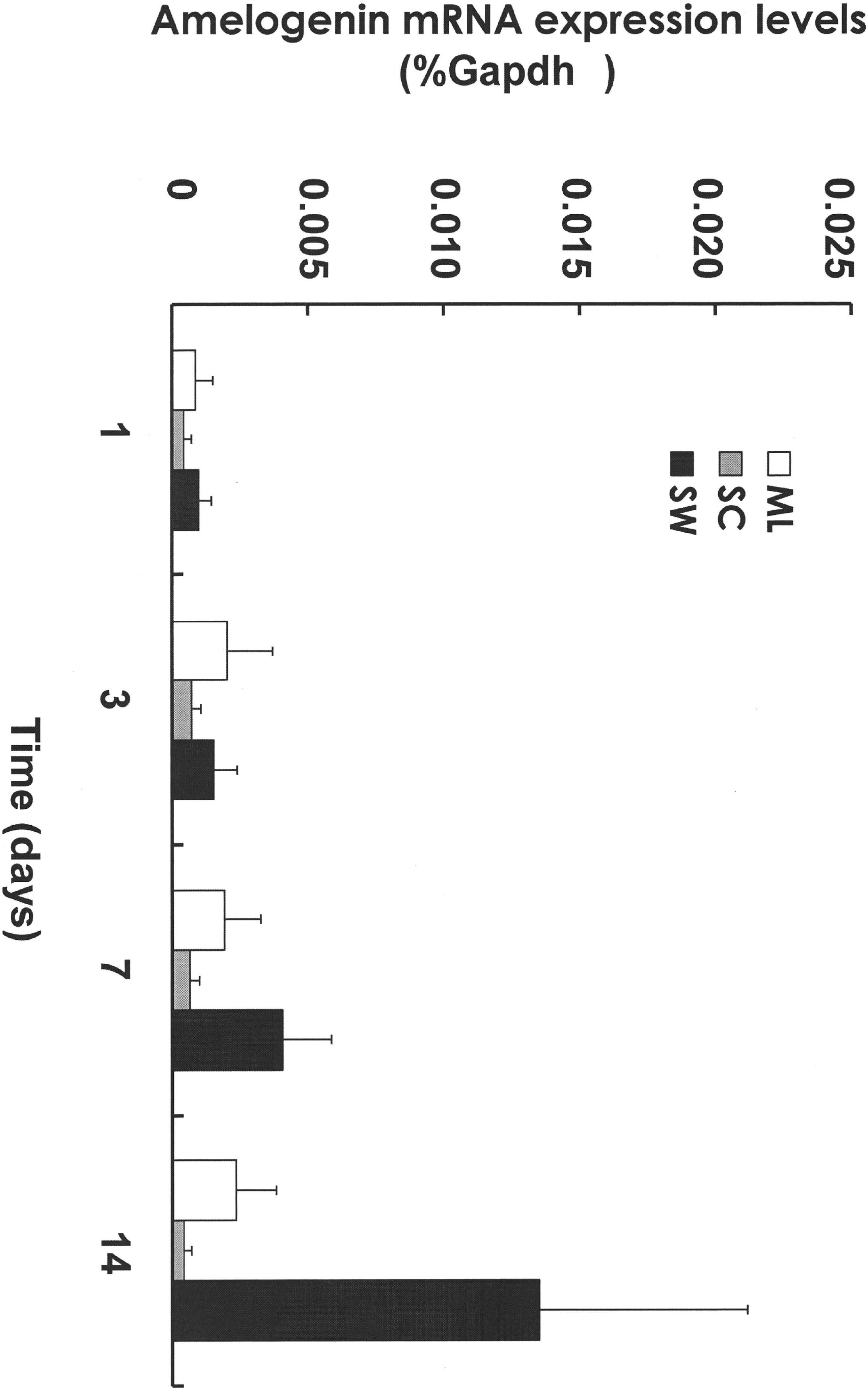
Amelogenin mRNA expression levels
(%Gapdh)
0
0.005
0.010
0.015
0.020
0.025
ML
SC
SW
1
3
7
14
Time (days)

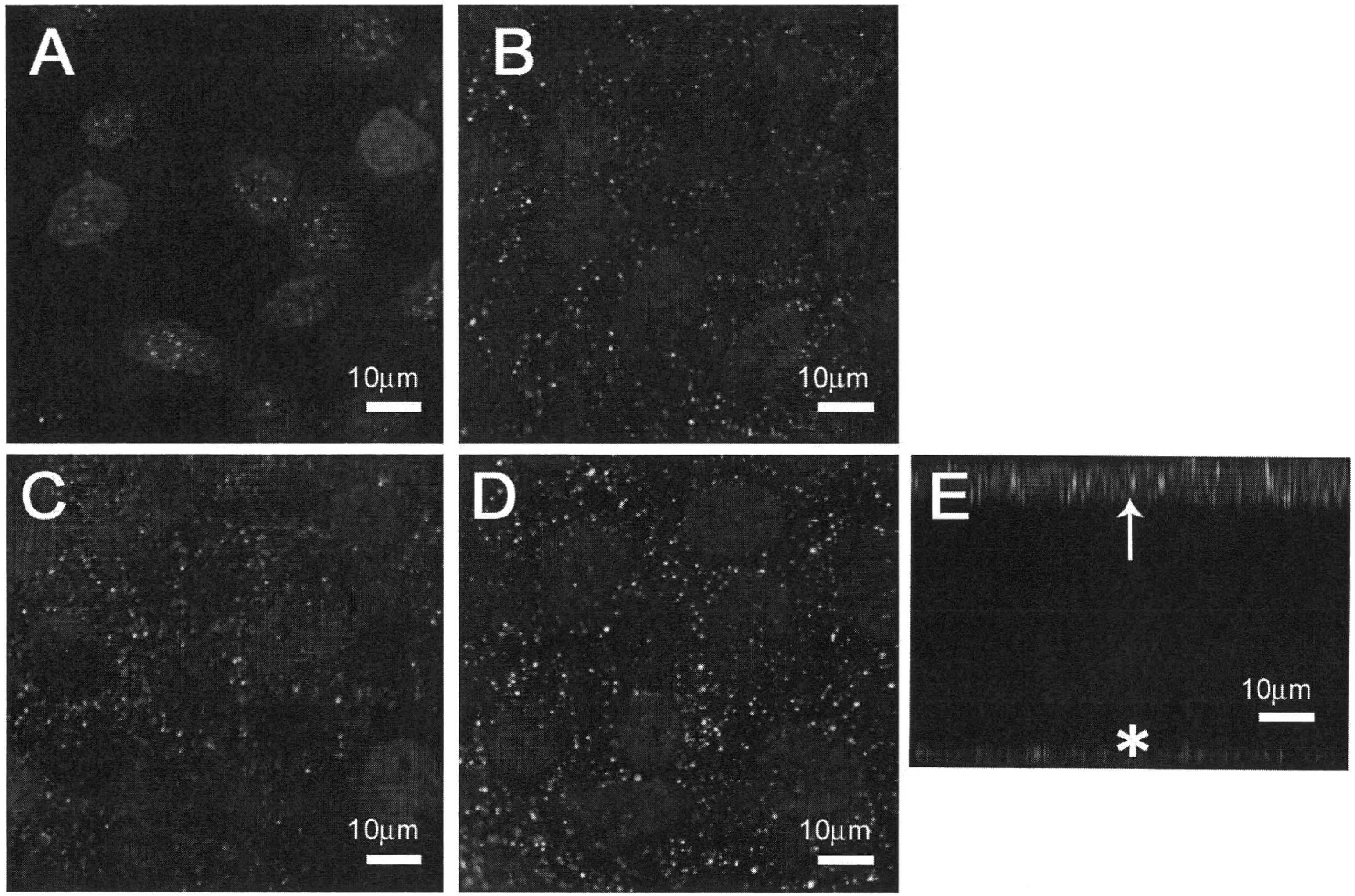

Fig.4 by Matsumoto et a

"Tooth regenerative therapy" as an organ replacement regenerative therapy

Masahiro Saito[1], Takashi Tsuji[2,3]
[1] Faculty of Industrial Science and Technology, Tokyo University of Science
[2] Research Institute for Science and Technology, Tokyo University of Science
[3] Organ Technologies Inc.

Keyword: regenerative therapy, tooth regeneration, organ germ method, tooth germ

Development of regeneration therapy is expected as a novel medical therapeutic system in 21th century. Tooth is developed from tooth germ which generated by epithelial-menechymal interactions during embryonic stage, and is a highly organized organ comprising several kinds of cells forming tooth and periodontium, mineralized tissues and blood vessels. Tooth regeneration has been developed as a model for organ replacement therapy that can replace the lost or damaged organ after disease or injury using bioengineered organ.

Tooth regenerative therapy is a bioengineered organ replacement as a future regenerative therapy

Current approaches of regenerative therapy are transplantation of tissue-derived stem/progenitor cells into the site of the damaged tissue or organ. The ultimate goal of regeneration therapy is to develop a fully functioning bioengineered organ that can replace lost or damaged organ after injury, disease or aging.

Tooth is developed from a tooth germ, which generated by epithelial-menechymal interactions at embryonic stage, and is a highly organized organ comprising several kinds of cells forming tooth and periodontium, mineralized tissues and blood vessels. Current strategy for tooth regeneration is to reproduce a bioengineered tooth germ by the reconstitution of immature epithelial and mesenchymal cells isolated from developing tooth germ. Realization of tooth regeneration therapy is required for wide variety of technology development such as cell processing technology for reconstituting tooth germ, identification of cell seeds capable of reconstituting bioengineered tooth germ, and technology for the regulation of tooth size and morphology.

Development of a novel three-dimensional cell processing method "Organ Germ Method" for making bioengineered tooth germ

We have recently developed a three-dimensional single cell processing method, named as an organ germ method which can be reconstituted organ germ, as a first step for developing tooth regeneration therapy (fig.1). A bioengineered tooth germ was reconstituted using dissociated dental epithelial and mesenchymal cells with the correct cell compartmentalization at high-cell density in collagen gel. The bioengineered tooth germ could regenerate structurally correct tooth in subrenal capsule transplantation at high frequency (fig.2). The structurally correct tooth could also be regenerated from the bioengineered germ in an *in vitro* organ culture (fig.3).

Analysis of the development of the bioengineered tooth germ in adult oral environment

The bioengineered tooth germ could also generate a structurally correct tooth after the transplantation under a tooth cavity of adult mice showing penetrations of nerve fibers and blood vessels (fig.4). Our results demonstrate the potential of the bioengineered tooth replacement by the transplantation of the bioengineered tooth germ in adult oral environment for use in future organ replacement regenerative therapy.

Furthermore, we have been performed the feasibility study for the realization of tooth regeneration therapy in collaboration with dental research organizations. Further studies on the identification of adult tissue-derived cell seeds for the reconstitution of the bioengineered tooth germ, initiation signals for tooth development, and regeneration of periodontium and tooth root will help to achieve the realization of tooth regenerative therapy for missing tooth. These technical achievements will make substantial contributions to an improvement of quality of life for many people and the development of bioengineering technology for future organ replacement regenerative therapy.

Figure 1 Development of three-dimensional cell processing technology (bioengineered organ germ method) that can regenerate bioengineered tooth germ.

① Epithelial and mesenchymal tissues were isolated from incisor tooth germ of ED14.5 mice and then completely dissociated into epithelial and mesenchymal cells respectively.

② Epithelial and mesenchymal cells at high cell density were injected into collagen gel successively.

③ The bioengineered tooth germ was reconstituted using epithelial and mesenchymal cells with correct cell compartmentalization at high cell density.

切歯歯胚：incisor tooth germ, 上皮組織：epithelial tissues, 上皮細胞:：epithelial cells,間葉組織：mesenchymal tissues, 間葉細胞：mesenchymal cells

Figure 2 Development of bioengineered tooth germ under an *in vivo* subrenal capsule transplantation.

① Bioengineered tooth germ was incubated for several days with organ culture.

② Bioengineered tooth germ was transplanted into a subrenal capsule for 14 days.

③ Bioengineered tooth and alveolar bone with correct tooth structure were observed after 14-days transplantation in the subrenal capsule.

再生歯：Regenerated tooth. 再生歯槽骨：Regenerated alveolar bone
組織像：Histology, 血管：Blood vessels, 歯髄：Pulp, エナメル質：Enamel, 象牙質: Dentin, 象牙芽細胞：odontoblast

Figure 3 Development of the bioengineered incisor and molar tooth germ in *in vitro* organ culture.

① Bioengineered tooth germ was cultured for 14days in *in vitro* organ culture.

② Bioengineered tooth germ gave rise to form incisor and molar tooth from each bioengineered germs.

Figure 4 Bioengineered tooth was developed after the transplantation of the bioengineered tooth germ in the tooth cavity of adult mice.

① Reconstituted tooth germ was cultured for several days in an *in vitro* organ culture.

② Isolation of single bioengineered tooth germ by micro-surgery.

③ Transplantation of the bioengineered tooth germs into tooth cavity of adult mouse.

④ Histological analysis of tooth cavity without transplantation.

⑤ Histological analysis of the tooth cavity after 14-days transplantation of the bioengineered tooth germ.

References

1. K. Nakao, R. Morita, Y, Saji, K. Ishida, Y. Tomita, M. Ogawa, M. Saito, Y. Tomooka, T. Tsuji, The development of a bioengineered organ germ method. *Nature Method* **4** (10): 227-230, 2007
2. Komine A, Suenaga M, Nakao K, Tsuji T, Tomooka Y. Tooth regeneration from newly established cell lines from a molar tooth germ epithelium. *Biochem Biophys Res Commun.* **355**(3): 758-763, 2007

Profile

Masahiro Saito, DDS PhD
Associate Professor, Faculty of Industrial Science and Technology, Tokyo University of Science
2641 Yamazaki, Noda, Chiba 278-8510, Japan

Takashi Tsuji, PhD
Professor, Research Institute for Science and Technology, Tokyo University of Science
Director, Organ Technologies Inc.
2641 Yamazaki, Noda, Chiba 278-8510, Japan

We are working on technology development of tooth regeneration as model for generation of bioengineered organ by arrangement of three-dimensional cell culture system. In order to achieve these technologies, we conduct basic research jointly with dental research organizations.

Cell Tissue Res (2010) 341:381–395
DOI 10.1007/s00441-010-1021-5

REGULAR ARTICLE

Dilated capillaries, disorganized collagen fibers and differential gene expression in periodontal ligaments of hypomorphic fibrillin-1 mice

Ganjargal Ganburged · Naoto Suda · Masahiro Saito · Yosuke Yamazaki · Keitaro Isokawa · Keiji Moriyama

Received: 18 December 2009 / Accepted: 13 July 2010 / Published online: 17 August 2010

Abstract The periodontal ligaments (PDLs) are soft connective tissue between the cementum covering the tooth root surface and alveolar bone. PDLs are composed of collagen and elastic system fibers, blood vessels, nerves, and various types of cells. Elastic system fibers are generally formed by elastin and microfibrils, but PDLs are mainly composed of the latter. Compared with the well-known function of collagen fibers to support teeth, little is known about the role of elastic system fibers in PDLs. To clarify their role, we examined PDLs of mice under-expressing fibrillin-1 (mgR mice), which is one of the major microfibrillar proteins. The PDLs of homozygous mgR mice showed one-quarter of the elastic system fibers of wild-type (WT) mice. A close association between the elastic system fibers and the capillaries was noted in WT, homozygous and heterozygous mgR mice. Interestingly, capillaries in PDLs of homozygous mice were dilated or enlarged compared with those of WT mice. A comparable level of type I collagen, which is the major collagen in PDLs, was expressed in PDL-cells of mice with three genotypes. However, multi-oriented collagen fiber bundles with a thinner appearance were noted in homozygous mice, whereas well-organized collagen fiber bundles were seen in WT mice. Moreover, there was a marked decrease in periostin expression, which is known to regulate the fibrillogenesis and crosslinking of collagen. These observations suggest that the microfibrillar protein, fibrillin-1, is indispensable for normal tissue architecture and gene expression of PDLs.

Keywords Fibrillin-1 · Periodontal ligament · Periostin · Type I collagen · Sharpey's fibers · Mouse (mgR)

Funding This study was supported by Grant-in-Aid for Scientific Research from the Ministry of Education, Culture, Sports, Science, and Technology of Japan (No. 18390552, 19659547, and 21390546), by Sato Fund and Dental Research Center Grant at Nihon University School of Dentistry, and by Grant for Supporting Project for Strategic Research of Nihon University School Dentistry at Matsudo by the Ministry of Education, Culture, Sports, Science, and Technology of Japan.

G. Ganburged · N. Suda (✉) · K. Moriyama
Maxillofacial Orthognathics, Department of Maxillofacial Reconstruction and Function, Division of Maxillofacial/Neck Reconstruction, Graduate School of Medical and Dental Sciences, Tokyo Medical and Dental University,
1-5-45 Yushima, Bunkyo-ku,
Tokyo 113-8510, Japan
e-mail: n-suda.mort@tmd.ac.jp

G. Ganburged · N. Suda · K. Moriyama
Global Center of Excellence (GCOE) Program, International Research Center for Molecular Science in Tooth and Bone Diseases,
Tokyo, Japan

M. Saito
Research Institute for Science and Technology, Tokyo University of Science,
Chiba, Japan

Y. Yamazaki · K. Isokawa
Department of Anatomy, Nihon University School of Dentistry,
Tokyo, Japan

Y. Yamazaki · K. Isokawa
Division of Functional Morphology, Dental Research Center, Nihon University School of Dentistry,
Tokyo, Japan

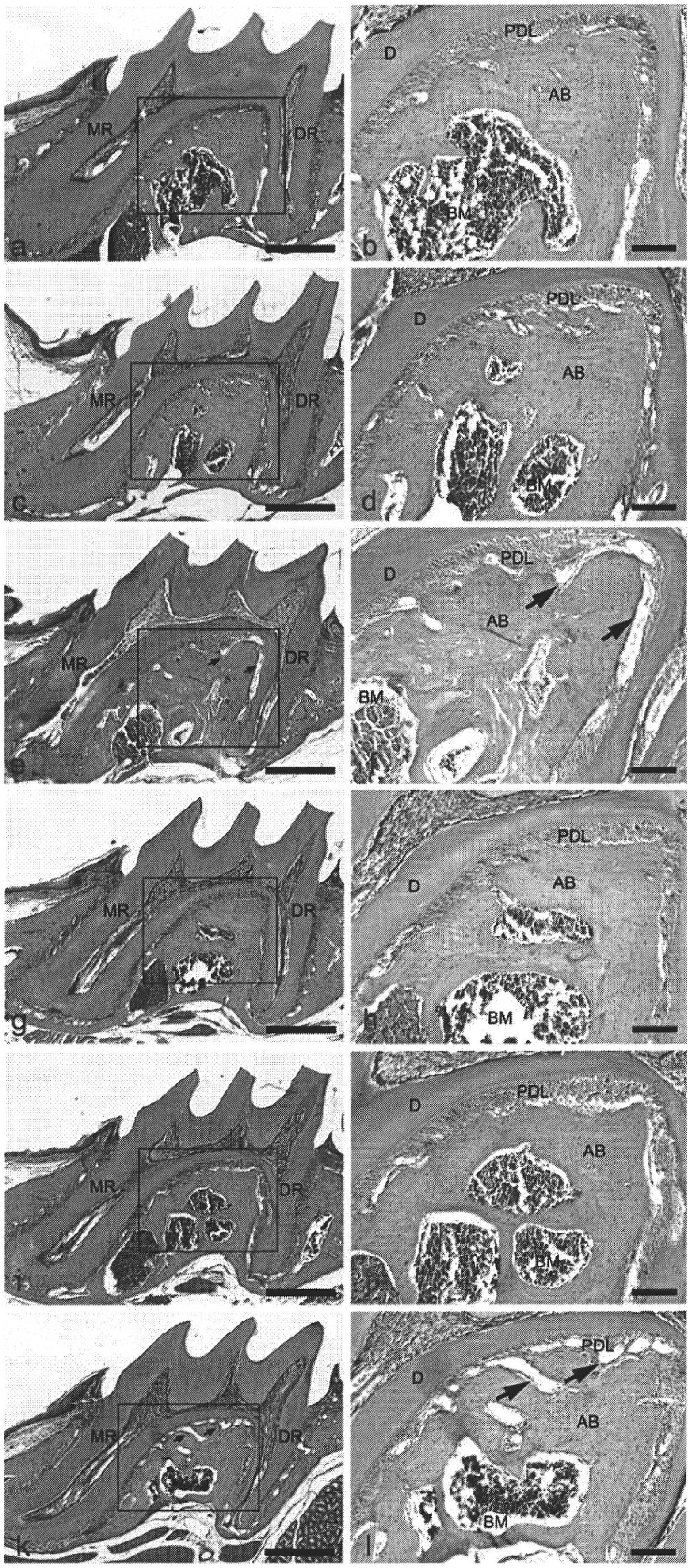

Fig. 1 Histological appearance of hematoxylin and eosin-stained sections around maxillary first molars in 2- (**a–f**) and 8-week-old (**g–l**) mice. WT (**a,b,g,h**), heterozygous (**c,d,i,j**), and homozygous (**e,f,k,l**) mice are shown. Higher magnifications of *boxed areas* in (**a,c,e,g,i,k**) are shown in (**b,d,f,h,j, l**), respectively. Note that many capillaries were present in the PDLs, and dilated capillaries (*arrows* in **e,f,k,l**) were noted in the homozygous mice but not in the other types of mice. This was more apparent in 8-week-old homozygous mice compared with those at 2 weeks. Magnification ×4 (**a,c,e,g,i,k**), ×10 (**b,d,f, h,j,l**). *AB* Alveolar bone, *BM* bone marrow, *D* dentin, *DR* distal root, *MR* mesial root, *PDL* periodontal ligament. *Bars* 400 μm (**a,c,e,g,i,k**), 100 μm (**b,d,f,h,j,l**)

Introduction

Periodontal ligaments (PDLs) are characteristic and specialized connective tissue, located between the socket of the alveolar bone and cementum covering tooth roots (Nanci 2007). PDLs are composed of fibers, blood vessels, nerves, and various kinds of cells. More than half of these structural elements are collagen fibers (Freezer and Sims 1987). Most of the collagen fibrils in PDLs are arranged in definite and well-organized fiber bundles. The termini of collagen fiber bundles of PDLs are at the end of the alveolar bone and cementum, and are termed as Sharpey's fibers.

The predominant collagens of PDLs are types I, III and XII. Among them, type I is the most abundant (Nanci 2007) and its expression becomes apparent in PDLs as root forms (MacNeil et al. 1998). Type XII collagen is seen in a relatively large amount in ligamentous tissues, including PDLs (Karimbux et al. 1992; Karimbux and Nishimura 1995; MacNeil et al. 1998). Type XII collagen belongs to the Fibril Associated Collagens with Interrupted Triple Helices (FACITs), having short triple-helical domains separated by non-triple-helical regions (Gordon et al. 1987; Shaw and Olsen 1991). A study of transgenic mice carrying a dominant interference mutation in type XII collagen [truncated $\alpha 1$ (XII)] indicated that this collagen plays an important role in the extracellular matrix architecture of PDLs (Reichenberger et al. 2000).

Periostin was originally termed osteoblast-specific factor-2 (Osf-2), and is known to exhibit structural similarity to a homophilic adhesion molecule, fasciclin-1 (Takeshita et al. 1993). This molecule is predominantly expressed in collagen-rich fibrous connective tissues. Periostin is expressed in PDLs, and accumulating evidence suggests that this molecule is required to maintain the integrity of PDLs (Afanador et al. 2005; Rios et al. 2005, 2008; Kii et al. 2006). Recently, periostin has been suggested to regulate the fibrillogenesis and crosslinking of collagens (Norris et al. 2007).

Elastic system fibers are widely distributed among various types of connective tissue where elasticity is required, such as the skin, lung, and blood vessels (Mecham 1991). These fibers are composed of elastin and microfibrils. Depending on the relative amount of elastin, they are classified as elastic, elaunin and oxytalan fibers (Kielty et al. 2002). Oxytalan fibers, which lack elastin, are made up of bundles of 10- to 12-nm microfibrils that are predominantly composed of glycoproteins, fibrillin-1 and -2. In PDLs, the main elastic system fibers are oxytalan fibers, which are oriented in an occluso-apical direction (Fullmer et al. 1974; Beertsen et al. 1997; Tashiro et al. 2002; Shiga et al. 2008; Suda et al. 2009; Tsuruga et al. 2009). There is also a small amount of elaunin fibers in the apical region (Staszyk and Gasse 2004; Sawada et al. 2006). It is known that mutation in the gene encoding fibrillin-1, *FBN1*, causes an autosomal dominant disorder Marfan syndrome type I (MFS1, MIM #154700), characterized by tall stature, aortic dissection, mitral valve prolapse and ectopia lentis (Pyeritz 2000). In addition to these conditions, severe periodontitis is frequently associated with this syndrome (De Coster et al. 2002)

Compared with collagen fibers, there is only limited information on elastic system fibers in PDLs. To clarify the function of elastic system fibers in PDLs, we examined PDLs in hypomorphic fibrillin-1 mice (mgR), which showed the reduction of *Fbn1* (encoding mouse fibrillin-1) expression as a result of transcriptional interference by insertion of the PGK*neo*-cassette (Pereira et al. 1999). Findings in this study showed the aberrant architecture of collagen fibers and differential gene expression of PDL-cells in mgR mice, suggesting that the microfibrillar protein, fibrillin-1, is indispensable for normal PDL development.

Materials and methods

Animals

Two- to eight-week-old male mgR mice were used in this study. We found that homozygous mgR mice could only survive for up to 3 or 4 months, as reported (Pereira et al. 1999). Thus, heterozygous mgR mice were mated to generate wild-type (WT), heterozygous, and homozygous mgR mice. Totals of 16 WT (6 at 2 weeks; 4 at 6 weeks; 6 at 8 weeks), 16 heterozygous (6 at 2 weeks; 4 at 6 weeks; 6 at 8 weeks), and 15 homozygous mgR (6 at 2 weeks; 3 at 6 weeks; 6 at 8 weeks) mice were used in this study. Experimental procedures were approved by the Experimental Animal Committee of Tokyo Medical and Dental University (No.100073).

Table 1 The sum of the capillary size in PDLs of WT, heterozygous and homozygous mgR mice

Genotype of mice	Mean	SE	*P* value
WT mice	976.8	172.1	-
Heterozygous mgR mice	2,010.4	228.4	$<0.01^{a}$
Homozygous mgR mice	2,892.5	231.9	$<0.001^{b}$

Each value is represented as μm^2. The mean and SE values were calculated from six different sections in each kind of genotype, as described in "Materials and methods". Eight-week-old mice were used for the evaluation

[a] WT versus heterozygous mgR mice

[b] WT versus homozygous mgR mice

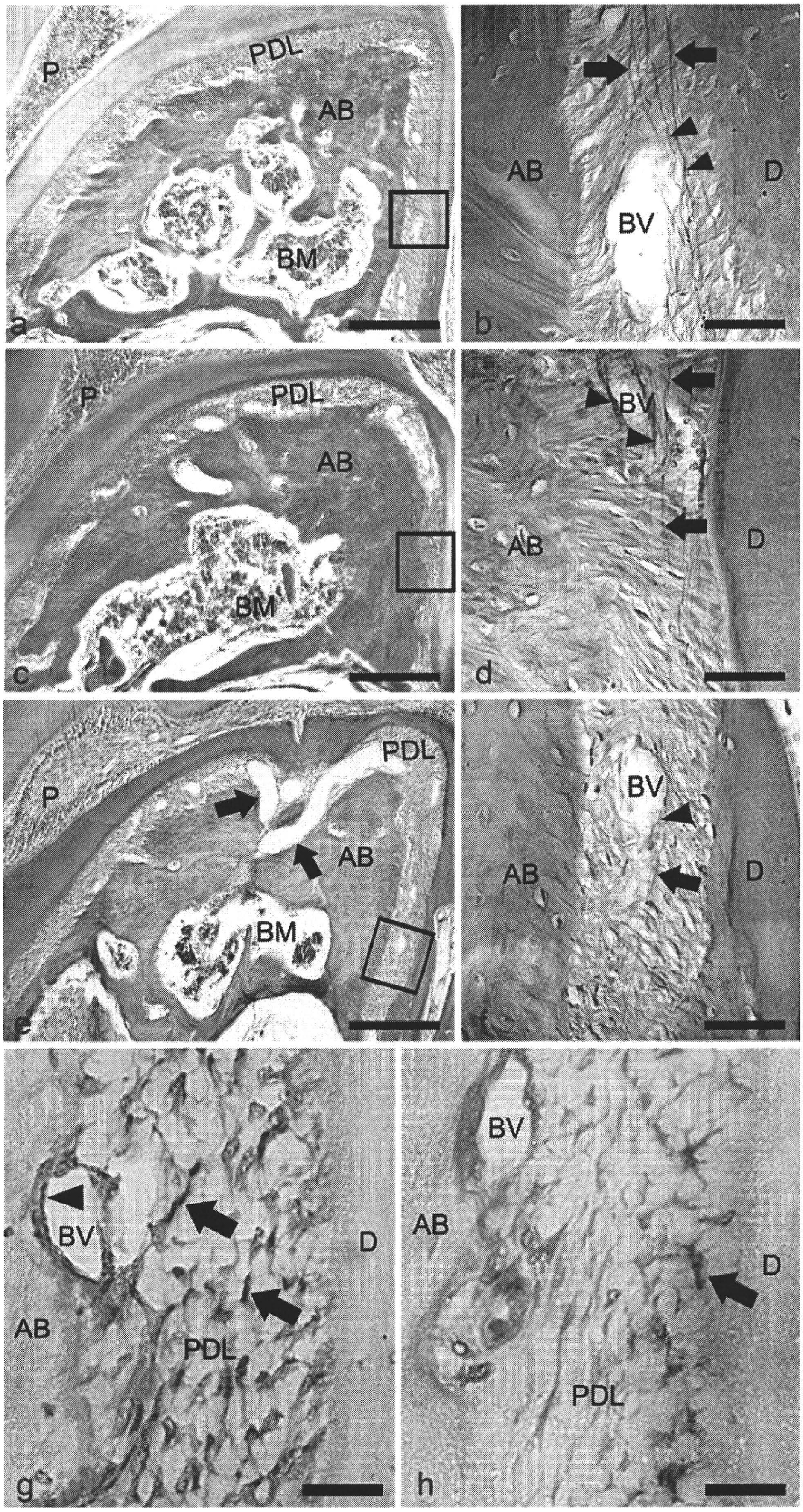

Fig. 2 Resorcin-Fuschin stained sections showing elastic system fibers around maxillary first molars of WT (**a**,**b**), heterozygous (**c**,**d**), and homozygous (**e**,**f**) mice at 2 weeks of age. Higher magnifications of *boxed areas* in (**a**,**c**,**e**) are shown in (**b**, **d**,**f**), respectively. Stained fibers (*arrows* in **b**,**d**) were clearly seen, and there was an association between the stained fibers and capillaries (*arrowheads* in **b**,**d**) in the WT and heterozygous mice. A lower amounts of elastic system fibers with a shorter appearance (*arrow* in **f**) were noted in the homozygous mice. Also, there were lower amounts of fibers showing an association with the capillaries (*arrowhead* in **f**) in the homozygous mice. Some dilated capillaries were noted in homozygous mice (*arrows* in **e**). In situ hybridization of fibrillin-1 in the PDLs of WT (**g**) and homozygous (**h**) mice. The expression was clearly seen in PDL-cells (*arrows* in **g**,**h**) of both genotypes, and there were lower numbers of fibrillin-1 expressing cells in homozygous mice than in WT mice. The expression was seen in endothelial cells (*arrowhead*) in WT mice but not in homozygous mice. Magnification ×10 (**a**,**c**,**e**), ×40 (**b**,**d**,**f**), ×60 (**g**,**h**). *AB* Alveolar bone, *BM* bone marrow, *BV* capillaries, *D* dentin, *PDL* periodontal ligament, *P* dental pulp. *Bars* 200 μm (**a**,**c**,**e**), 40 μm (**b**,**d**,**f**), 25 μm (**g**,**h**)

Table 2 Resorcin-fuchsin stained areas in PDLs of WT, heterozygous and homozygous mgR mice

Genotype of mice	Mean	SE	*P* value
WT mice	22.34	2.69	-
Heterozygous mgR mice	10.39	1.29	<0.001[a]
Homozygous mgR mice	5.33	0.70	<0.001[b]

Each value is represented as $\mu m^2/mm^2$. The mean and SE values were calculated from 18 different Resorcin-fuchsin stained areas in each kind of genotype, as described in "Materials and methods". Six-week-old mice were used for the evaluation

[a] WT versus heterozygous mgR mice

[b] WT versus homozygous mgR mice

Histological preparation

Mice were anesthetized with 50 mg/ml sodium pentobarbital and perfusion fixation was performed using 4% paraformaldehyde in 0.1 M phosphate buffer (PBS, pH 7.4) treated with diethylpyrocarbonate (DEPC). Maxillae were dissected and decalcified in Morse solution (10% sodium citrate, 20% formic acid, Wako, Japan) for one week, and dehydrated and embedded in paraffin (Wako). Five-µm-thick serial sagittal sections of the maxillary molars with surrounding tissue were prepared for light-microscopic observation. Some sections were deparaffinized and stained by hematoxylin (Muto Pure Chemicals, Japan) and 0.5% eosin Y ethanol (Wako) solution.

To visualize the elastic system fibers, sections were stained by Resorcin-fuchsin solution (Muto Pure Chemicals) after 10% oxone (Wako) treatment and counterstained by 1% Orange G (Wako). With oxone treatment, both elastin and microfibrils can be visualized.

Picrosirius polarization staining

To highlight collagen fibers in PDLs, sections were stained with Picrosirius red solution (Muto Pure Chemicals) and washed in 0.005% acetic acid solution before mounting on cover slides. Collagen orientation was observed three dimensionally, using a polarizing light microscope (Eclipse LV100 POL; Nikon, Japan). Details of collagen orientation have been described by Rieppo et al. (2008).

In situ hybridization

Both the sense and antisense digoxigenin-11-uridine triphosphate (DIG-11-UTP)-labeled single-stranded RNA probes of *Col12a1* (encoding mouse type XII collagen), *Fbn1* (encoding mouse fibrillin-1), and *postn* (encoding mouse periostin) were prepared using a DIG RNA labeling kit (Roche, Indianapolis, IN, USA) according to the manufacturer's instructions. The template cDNA was a 503-bp *Spe* I-*Not* I fragment of *Col12a1* (corresponding to 7152-7654 in NM_007730), a 522-bp *Spe* I-*Not* I fragment of *Postn* (corresponding to 11-532 in NM_015784), and a 500-bp *Spe* I-*Not* I fragment of *Fbn1* (corresponding to 6952-7451 in NM_007993). The template cDNA of *Col1a1* (encoding mouse type I collagen) was cloned by reversed transcription-PCR, according to the website of the Allen Institute for Brain Science (http://mouse.brain-map.org/brain/Col1a1/71992079.html?ispopup=true), and labeled by a DIG RNA labeling kit. The hybridization procedure was carried out as previously described (Suda et al. 2001). Briefly, deparaffinized sections were treated with proteinase K at 37°C, followed by hybridization with a DIG-labeled probe for 16 h at 60°C. After hybridization, slides were washed to remove unbound probes. The DIG-labeled probes were detected using a nucleic acid detection kit (Roche) according to the manufacturer's instructions. Sections were counterstained with 0.5% eosin Y ethanol solution (Wako).

Immunostaining

Immunostaining of von Willebrand factor (ADAMTS13) was performed by using the rabbit polyclonal antibody against human von Willebrand factor (Novus Biologicals, Littleton, CO, USA). The goat anti-rabbit IgG antibody conjugated to horseradish peroxidase (HRP) (Novus Biologicals) was used as a second antibody, and a color detection was performed by using diaminobenzidine (DAB). Immunostaining of PECAM-1 (CD31) was performed by using the rat monoclonal antibody against mouse PECAM-1 (Santa Cruz Biotechnology, Santa Cruz, CA, USA) and the rat ABC staining system (Santa Cruz Biotechnology), according to the manufacturer's instruction. All sections were counterstained with 0.05% toluidine blue solution and visualized under light microscopy.

Apoptotic cells in PDLs

To examine the TUNEL (TdT-mediated dUTP-biotin nick end labeling)-positive apoptotic cells around capillaries in PDLs, in situ cell death detection kit (Roche) was used, according to the manufacturer's instruction.

Electron-microscopic observation

Ultrathin sections of 6-week-old mice were prepared from embedded (Epon 812; TAAB, England) specimens. Sections were prepared from an identical level of each root (at the middle of each root length). The sections were contrasted with 2.5% uranyl acetate and Sato's lead salts (Sato 1968), and examined with a transmission

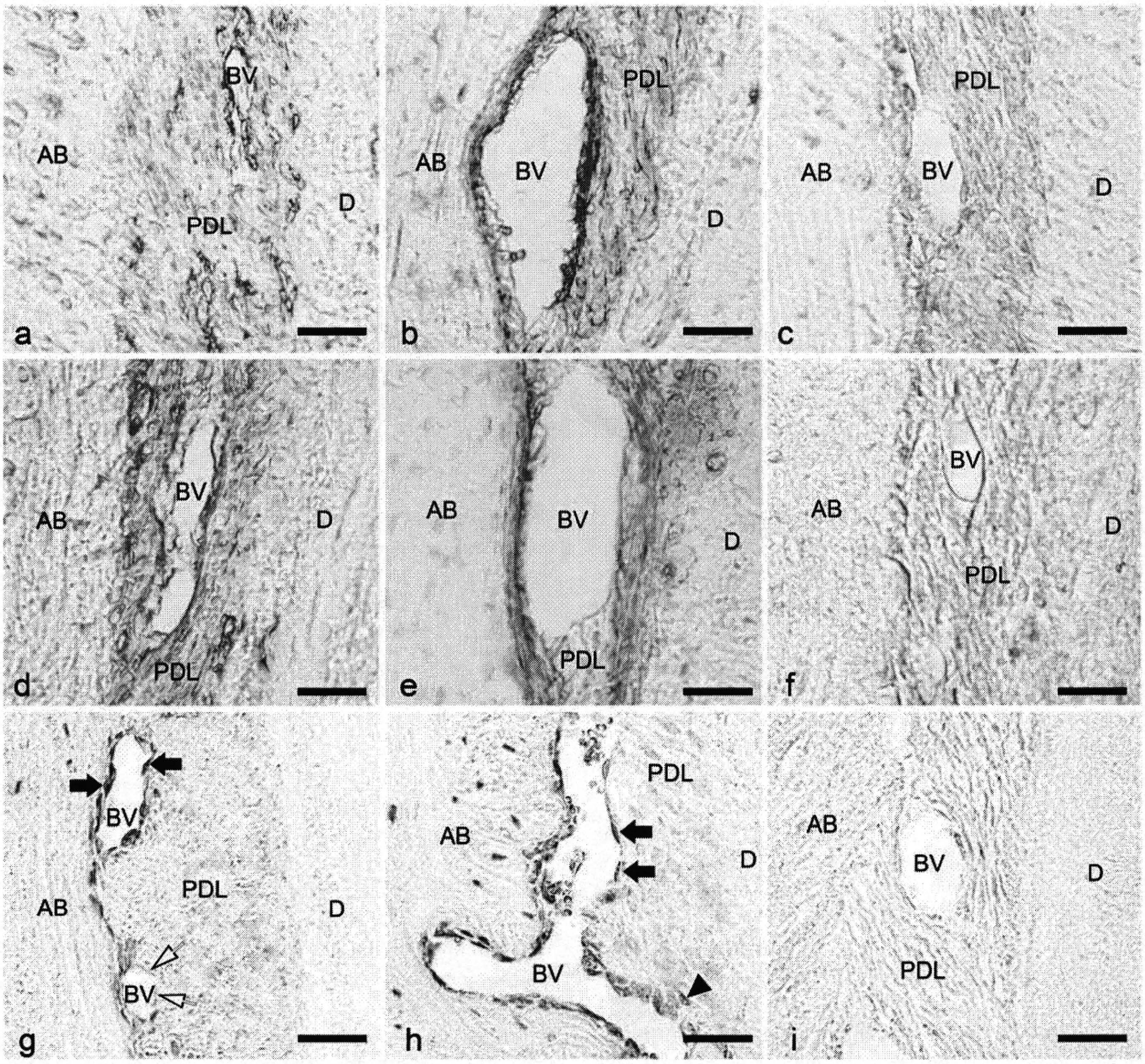

Fig. 3 Immunolocalization of PECAM-1 (CD31) (**a–c**) and von Willebrand factor (**d–f**) in the PDLs of 8-week-old mice. Sections of WT (**a,c,d,f**) and homozygous (**b,e**) mice. The immunoreaction of PECAM-1 and von Willebrand factor was seen in endothelial cells of WT (**a,d**) and homozygous mgR mice (**b,e**). The negative controls, in which the rabbit polyclonal antibody against von Willebrand factor was replaced with the normal rabbit serum (**c**), and the rat monoclonal antibody against mouse PECAM-1 was replaced with the rat Ig (**f**), are shown. The TUNEL-staining of the PDLs in WT (**g,i**) and homozygous mice (**h**) at 8 weeks of age. The section of WT mouse without using the terminal deoxynucleotidyl transferase is shown in (**i**). TUNEL-positive cells were seen around capillaries in both WT (**g**) and homozygous mice (**h**). There were larger numbers of TUNEL-positive cells around capillaries of homozygous mice than in WT mice. Magnification ×40; *black arrows* TUNEL-positive endothelial cells, *white arrows* TUNEL-negative endothelial cells, *arrowhead* fibroblastic cell, *AB* alveolar bone, *BV* capillaries, *D* dentin, PDL periodontal ligament. *Bars* 20 μm

electron microscope (H-800; Hitachi, Tokyo, Japan) at an accelerating voltage of 75 kV.

Statistical analysis

To compare the capillary size of PDLs in WT, heterozygous and homozygous mgR, sagittal sections (7-μm-thick) were prepared from the maxillary first molars of each 8-week-old mouse. Three mice were used for each genotype. Two sections were prepared from the middle of the buccal and lingual dimension of each tooth root. The sum of the capillary sizes were evaluated in two unoverlapped rectangular areas in PDLs (two 750 μm × 100 μm rectangular areas in the bifurcation and in the mesial

Table 3 The number of TUNEL- positive cells around capillaries in PDLs

Genotype of mice	Mean	SE	*P* value
WT mice	0.43	0.06	
Homozygous mgR mice	1.12	0.11	< 0.001[a]

Each value is represented as cells/mm^2. The mean and SE values were calculated around 24 different capillaries in each genotype, as described in "Materials and methods". Eight-week-old mice were used for the evaluation

[a] WT versus homozygous mgR mice

side of the distal root, in each section). The ANOVA and Fisher's PLSD test were used to examine the differences between the WT, heterozygous, and homozygous mgR mice.

To compare the amount of elastic system fibers in WT, heterozygous and homozygous mgR mice, cross sections (7-μm-thick) of the distal sides of the distal roots were prepared from the maxillary first molars of each 6-week-old mouse. Three mice were used for each genotype. Two sections were prepared from an identical level of each root (at the middle of each root length) and stained by Resorcin-fuchsin solution with oxone pretreatment. Stained areas were evaluated in three randomly chosen areas in each section. A total of 18 areas were used for each genotype. ImageJ (ver.1.4.3; National Institutes of Health, MD, USA) was used for measuring Resorcin-fuchsin stained areas. The ANOVA and Steel-Dwass test were used to examine the differences between WT, heterozygous, and homozygous mgR mice.

To compare the number of apoptotic cells around capillaries in PDLs between WT and homozygous mgR mice. Four mice were used for each genotype. Two sections were prepared from the middle of the buccal and lingual dimension of the maxillary first molars in each 8-week-old mouse. Three capillaries were randomly chosen in the mesial side of the distal root in each section. A total of 24 capillaries were used for each genotype. The number of TUNEL-positive cells were counted in areas within 5 μm from each capillary. The Student's *t* test was used to examine the difference in the cell numbers between the WT and homozygous mgR mice. All statistical analyses were carried out with R (ver.2.10.0; R Foundation for Statistical Computing, Austria). *P* values less than 0.05 were considered significant.

Results

The histological appearances of the upper first molars and periodontal tissues of WT, heterozygous, and homozygous mgR mice are shown in Fig. 1. The appearance of the crown and root shape did not differ among the mice with three genotypes at 2 (Fig. 1a–f) or 8 (Fig. 1g–l) weeks old. A comparable thickness of PDLs was seen in mice with three genotypes, and bone marrows were similarly under the bifurcation areas (Fig. 1b, d, f, h, j, l). In both 2- and 8-week-old mice, numerous capillaries were seen in the PDLs. Dilated capillaries were noted in homozygous mice (Fig. 1f, l) but not in the other two types of mice. This was more apparent in 8-week-old homozygous mice (Fig. 1l) compared with those at 2 weeks old (Fig. 1f). The quantitative analysis of capillaries in the PDLs showed that the sum of capillary sizes in the heterozygous (2,010.4 μm^2) and homozygous (2,892.5 μm^2) mgR mice were significantly larger than that of WT mice (976.8 μm^2) (Table 1).

To highlight the elastic system fibers in PDLs, Resorcin-fuchsin staining was performed in 2-week-old mice with the three genotypes (Fig. 2). Fibers positive for this staining ran vertically in the PDLs of the three types of mice (Fig. 2b, d, f). There were many linear staining patterns in the WT and heterozygous mgR mice, and an association between elastic system fibers and capillaries was noted (Fig. 2b, d). In homozygous mice, there was a marked decrease in the amount of elastic system fibers, and fibers were shorter than those in WT and heterozygous mice (Fig. 2f). Additionally, there were fewer fibers showing an association to capillaries in homozygous mice than in the other two types of mice. All these stainings were performed by oxone treatment to visualize both elastin and microfibrils. Without oxone treatment, it is known that elastin but not microfibrils can be stained (Fullmer et al. 1974). PDLs were minimally stained without oxone treatment (data not shown), indicating that the majority of elastic system fibers in the mouse PDLs were microfibrils. Quantitative analysis of the amount of elastic system fibers in PDLs showed that there was a significant reduction in heterozygous (53.5% reduction to 10.39 μm^2/mm^2) and homozygous (76.1% reduction to 5.33 μm^2/mm^2) mice, compared to WT mice (22.34 μm^2/mm^2) (Table 2). In situ hybridization was performed to examine mRNA expression of fibrillin-1 in PDLs of the WT (Fig. 2g) and homozygous mgR (Fig. 2h) mice. The expression was clearly seen in PDL-cells of both genotypes, but there were lower numbers of fibrillin-1 expressing cells in homozygous mice than in WT mice. As reported in human endothelial cells (Vehviläinen et al. 2009), the expression was seen in endothelial cells of WT mice (Fig. 2g). But it was scarcely seen in endothelial cells of homozygous mgR mice (Fig. 2h).

Endothelial cells were immunostained by using specific antibodies against PECAM-1 (CD31) and von Willebrand factor (Fig. 3). The observation showed that immunoreaction against these antibodies was clearly seen in the

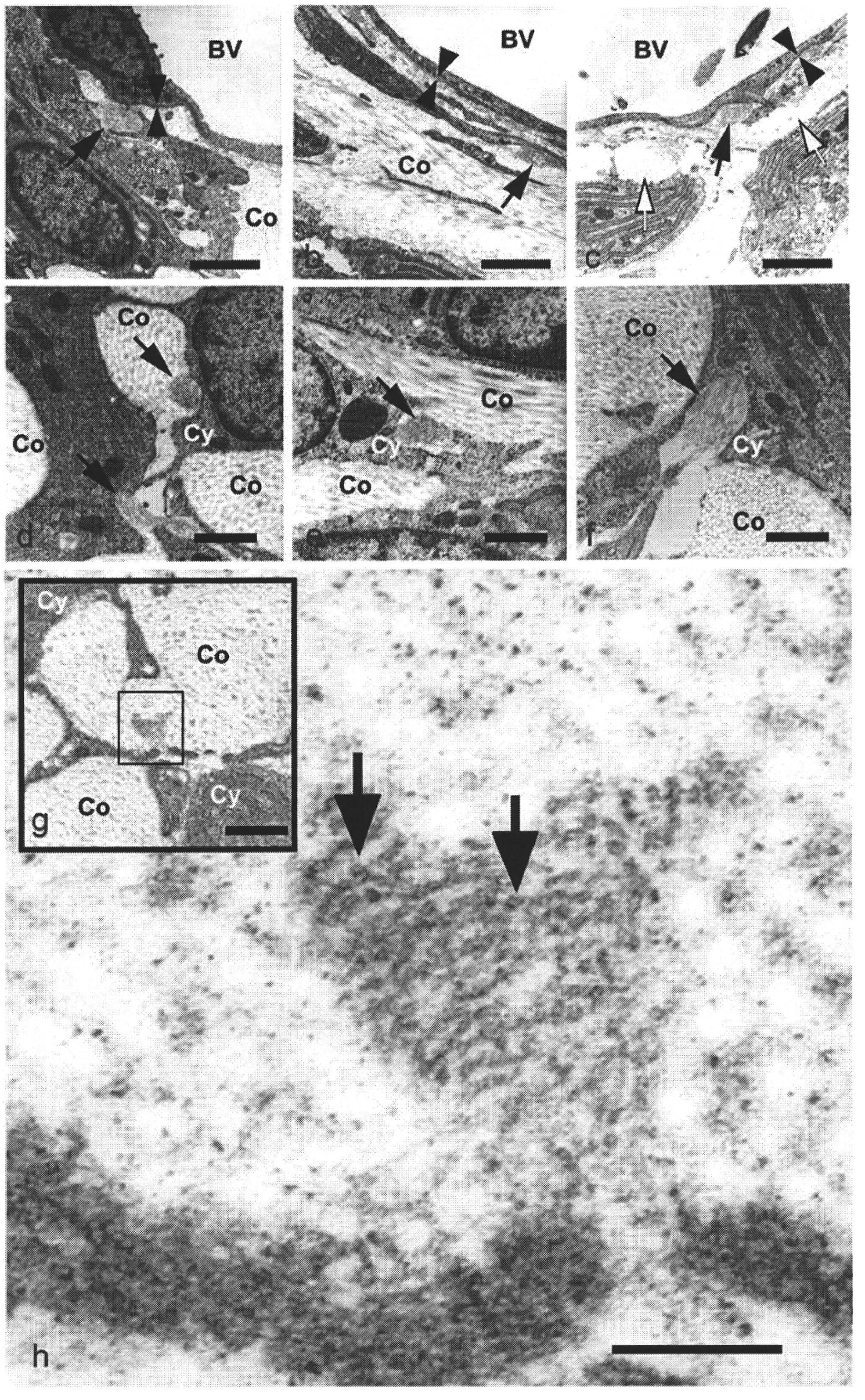

Fig. 4 Electron-microscopic observation of the PDLs of WT (**a,d,g,h**), heterozygous (**b,e**), and homozygous (**c,f**) mice. Sections around (**a–c**) and not around (**d–h**) the capillaries (*BV*) are shown. Bundles of microfibrils (*black arrows* in **a–f,h**) lacked any apparent amorphous appearance of elastin deposition and showed tubular structure (*black arrows* in **h**), indicating that there were elastin-free microfibrils. Note that each bundle of microfibrils (*black arrows* in **d–f**) was exclusively located adjacent to the PDL-cells and seen between the cytoplasmic processes. Degenerative cells (*white arrows* in **c**) were noted around capillaries in the homozygous mice, but scarcely seen in the heterozygous and never seen in the WT mice, respectively. Microfibrils were seen close to the basement membranes (*double arrowheads* in **a–c**). The *boxed area* in **g** is shown at higher magnification in **h**. *Co* Collagen, *Cy* cytoplasmic process. Magnification ×10,000 (**a–c**), ×18,000 (**d–g**), ×54,000 (**h**). *Bars* 5 nm (**a–c**), 2.5 nm (**d–g**), 0.5 nm (**h**)

endothelial cells of WT (Fig. 3a, d) and homozygous mgR mice (Fig. 3b, e). There were no stained cells in negative controls in which specific primary antibodies did not react (Fig. 3c, f). Next, apoptotic cells were examined by TUNEL staining (Fig. 3g–i). The TUNEL-positive cells were seen around capillaries both in the WT (Fig. 3g) and homozygous mgR mice (Fig. 3h). The endothelial cells in WT mice were both positive and negative to TUNEL

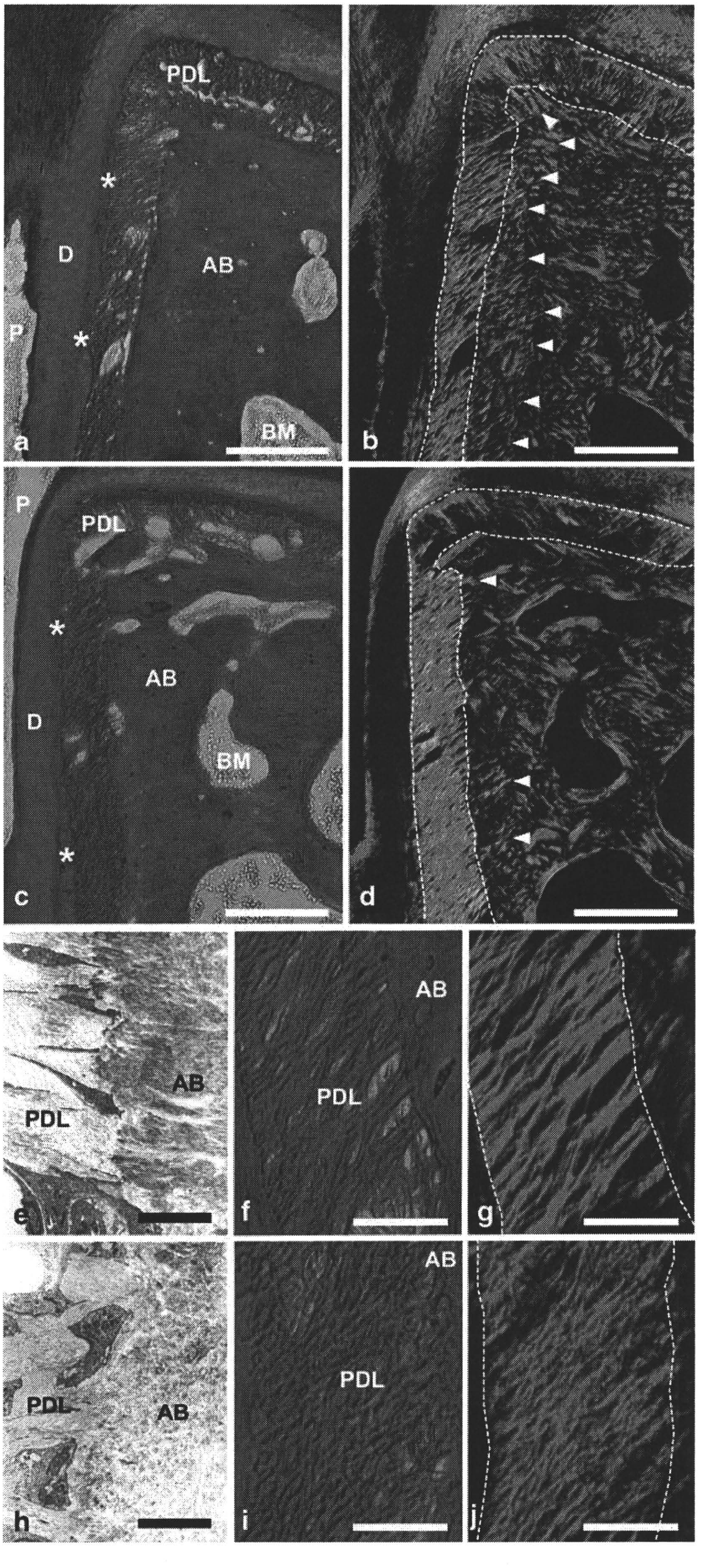

Fig. 5 Histological appearance of the PDLs in Picrosirius polarization staining sections of two-week-old mice (—**d**,**f**,**g**,**i**,**j**). Electron microscopic observation of the interface between the PDLs and the alveolar bones (**e**,**h**). Sections of WT (**a**,**b**,**e**–**g**) and homozygous (**c**,**d**,**h**–**j**) mice. Sections observed under transmission (**a**,**c**,**f**,**i**) and polarizing light (**b**,**d**,**g**,**j**) microscopy are shown. Stained collagen fibers that were perpendicular to the polarizing light are only visible in sections. Note that many Sharpey's fibers (*white arrowheads* in **b**) extended from the PDLs into the alveolar bone were seen in WT mice. There were apparently less visible Sharpey's fibers in homozygous mice (*white arrowheads* in **d**). The Sharpey's fibers ran in similar directions in the alveolar bone of the WT mice (**e**), but they were aligned in multi-directions in the homozygous mice (**h**). Compared with packed and well-organized collagen fiber bundles in the PDLs of the WT mice (**f**,**g**), homozygous mice (**i**,**j**) showed multi-oriented and disorganized collagen fiber bundles with a thinner appearance. Magnification ×25 (**a**–**d**), ×4,200 (**e**,**h**), ×100 (**f**,**g**,**i**, **j**). *AB* Alveolar bone, *BM* bone marrow, *D* dentin, *P* dental pulp, *PDL* periodontal ligament (indicated between two *dotted lines* in **b**,**d**,**g**,**j**), *Cementum. *Bars* 100 μm (**a**–**d**), 20 nm (**e**,**h**), 2.5 μm (**f**,**g**,**i**,**j**)

staining (Fig. 3g). In contrast, most of endothelial cells in homozygous mgR mice were TUNEL-positive, and there were larger number of TUNEL-positive cells around capillaries in homozygous mgR mice than in WT mice (Fig. 3h). The quantitative analysis showed that there were 2.6-fold higher number (0.43 cells/mm^2 and 1.12 cells/mm^2 in WT and homozygous mgR mice, respectively) of TUNEL-positive cells in homozygous mgR mice than in WT mice (Table 3).

Electron-microscopic observation of the PDLs showed that the bundle of microfibrils lacked an amorphous core of elastin deposition and showed the tubular structure, revealing that there were elastin-free microfibrils in three different genotypes of mice (Fig. 4). Microfibrils were observed close to basement membranes around the capillaries in the PDLs (Fig. 4a–c). Interestingly, there were destructed or degenerated cells specifically around the capillaries of homozygous mice (Fig. 4c). However, those kinds of cells were scarcely seen in heterozygous and not seen at all in WT mice (Fig. 4a, b). The relationship between microfibrils and PDL-cells is shown in Fig. 4d–f. Bundles of microfibrils were exclusively located adjacent to PDL-cells and seen between cytoplasmic processes of the three genotypes, suggesting a close association between cells and microfibrils in PDLs.

Next, the architecture of collagen fibers in the PDLs was examined by Picrosirius polarization staining under polarizing light microscopy (Fig. 5). In this method, stained collagen fibers that are perpendicular to the projected light are only visible under polarizing light microscopy. Under the transmission and polarizing light microscopy, definite and well-organized collagen fiber bundles ran from the cementum to the alveolar bone, and many Sharpey's fibers extended from the PDLs into the alveolar bone and cementum in the WT mice (Fig. 5a, b). There were less visible Sharpey's fibers in the alveolar

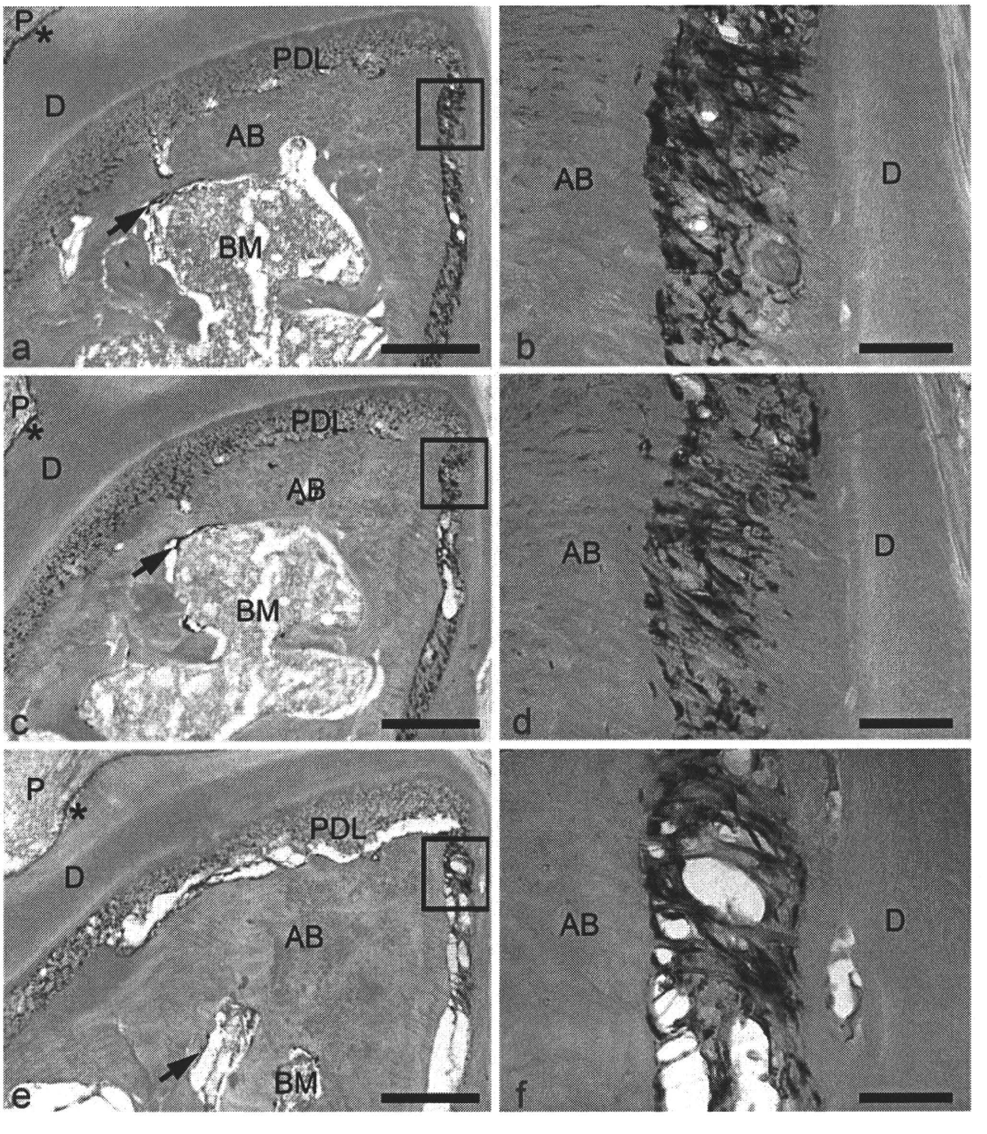

Fig. 6 In situ hybridization of type I collagen in WT **(a,b)**, heterozygous **(c,d)**, and homozygous **(e,f)** mice at 2 weeks of age. Higher magnifications of the *boxed areas* in **(a,c,e)** are shown in **(b,d,** f), respectively. Expression was noted in the cells of the PDLs, odontoblastic cells aligning on the dentin (*), and cells located in the most outer layers of the marrow cavities (*arrows*) in mice. Note that comparable expression was seen in the mice of three genotypes. *AB* Alveolar bone, *BM* bone marrow, *D* dentin, *P* dental pulp, *PDL* periodontal ligament. Magnification ×10 **(a,c,e)**, ×40 **(b,d,f)**. *Bars* 200 μm **(a,c,e)**, 40 μm **(b,d,f)**